Paper: ASAT-14-209-TH

14th International Conference on
AEROSPACE SCIENCES & AVIATION TECHNOLOGY,
ASAT - 14 – May 24 - 26, 2011, Email: asat@mtc.edu.eg
Military Technical College, Kobry Elkobbah, Cairo, Egypt
Tel: +(202) 24025292 –24036138, Fax: +(202) 22621908

Numerical Study of Film Cooling Over Flat Plate

A.S.Baher-Eneel*, A.F. El-Sayed†, M.H. Khobeiz‡

Abstract: The effect of film cooling over flat plate was investigated using Fluent 6.32. The computational domain included the coolant supply tube as well as the main mixing region. A tube L/D of 4 and injection angles of (30o, 60o, and 90o) were employed for blowing ratio of (0.33, 0.5, and 1.67), and a density ratio of 1.14. Adiabatic film cooling effectiveness distributions were also determined for inline and stagger arrangements. The main observation from this study that the 30o hole gave larger effectiveness values than 60o and 90o at the blowing ratio of 0.33 with the same length-to-diameter ratio. The maximum effectiveness was achieved with a blowing ratio of 0.5. The results show that the increase of blowing ratio negatively affects film cooling, such that for the blowing ratio of 1.67 the injected coolant tends to lift off from the wall due to the increase of the wall normal momentum. The comparisons for numerical results with experimental data are presented.

Keywords: Film cooling, Adiabatic effectiveness, Injection angle, Blowing ratio

Nomenclature

D	Hole diameter
h	Enthalpy
L	Hole length
M	Blowing ratio ($\frac{\rho_c v_c}{\rho_m v_m}$)
T_m	Main stream temperature
T_{aw}	Adiabatic wall temperature
T_c	Coolant temperature
x	Streamwise direction
v_c	Coolant velocity
v_m	Main stream velocity
ρ_c	Coolant density
ρ_m	Main stream density
η	Adiabatic effectiveness

* Libyan postgraduate student, www.baher_31@yahoo.com
† Prof. of Aerospace and Mechanical Engineering, Zagazeeg University, Egypt.
‡ Egyptian Armed Forces, Egypt.

Introduction

The advance of turbine engine technology has led to higher turbine inlet temperatures. This requires active cooling in order to maintain the blades of the turbine engine at a safe temperature, since the excessive high temperature levels will reduce the life of blades and can even cause the failure of those blades. Film cooling is a widely used technique to achieve this goal. Due to the large number of influence parameters, design optimization through experiments can be quite expensive and time consuming,

Consequently a reliable computationally efficient predictive procedure would be extremely beneficial. Even for a row of holes, the flow field is quite complex with a wide variety of influences parameters such as hole injection angle, hole diameter and shape, blowing ratio, lateral spacing, and the effect of the length of the coolant supply tube. FLUENT6.3 was used to solve the flow field and properties through the different configurations. Temperature contours, average effectiveness values and effectiveness contours has been presented using the same package. For the present study, CFD simulation for film cooling air flow along the tested flat plate is used, and the obtained numerical results are compared with experimental data.

Governing Equations

Continuity (Mass Conservation) Equation

It governs mass flow rates into and out of the computational volumes and the rate of accumulation of mass inside each volume. Then the continuity equation can be easily formulated as:

$$\nabla.\left(\rho.\vec{v}\right)=0 \tag{1}$$

Momentum Conservation Equations

Govern the flow velocities in and out of each control volume, and the associated forces acting on each. Hence the conservation of momentum in an inertial (non-accelerating) reference frame may described by:

$$\nabla.\left(\rho.\vec{v}\vec{v}\right)=-\nabla p+\nabla.(\bar{\tau})+\vec{F} \tag{2}$$

where:

p	static pressure.
$\bar{\tau}$	shear stress tensor.
$\vec{F}$	body force.

Energy Conservation Equation

It governs the different forms of energy and their transformation from one form to another. The total energy of a fluid particle (control volume) is defined as:

$$E=h-\frac{p}{\rho}+\frac{v^2}{2} \tag{3}$$

Turbulence Modeling Equations

These are several equations modeling the turbulence; in the present study, k-ε model is chosen. The standard k - ε model is a semi-empirical model based on model transport equations for the turbulence kinetic energy (k) and its dissipation rate (ε). The turbulent viscosity, μ_t, is computed by combining k and ε as follows:

$$\mu_t = \rho C_\mu \frac{k^2}{\varepsilon} \tag{4}$$

where C_μ is a constant.

When the segregated solver technique is incorporated, the governing equations are solved sequentially. This algorithm requires several iterations to obtain a converged solution due to the inherent non-linearity in the governing equations. The number of iterations would naturally increase if there are coupled equations as is the case when a turbulence model closure is used.

Adiabatic Effectiveness

The adiabatic film cooling effectiveness is defined as follows:

$$\eta = \frac{T_m - T_{aw}}{T_m - T_c} \tag{5}$$

where, T_{aw} denotes to the adiabatic wall temperature. The effectiveness value of 1.0 denotes that the adiabatic wall temperature is the same as the coolant temperature which implies that the wall is perfectly protected by the coolant.

Numerical Model

The flat plate to be film is illustrated in figure 1. The geometry of numerical model is as follows:

- The plate is 360mm wide ×1000mm long ×163mm thick.
- Hole diameter (D) = 10mm.
- Pitch to diameter is 3.
- Injection angles $30^{0,}$ 60^0, and 90^0.

Table 1 shows test cases data.

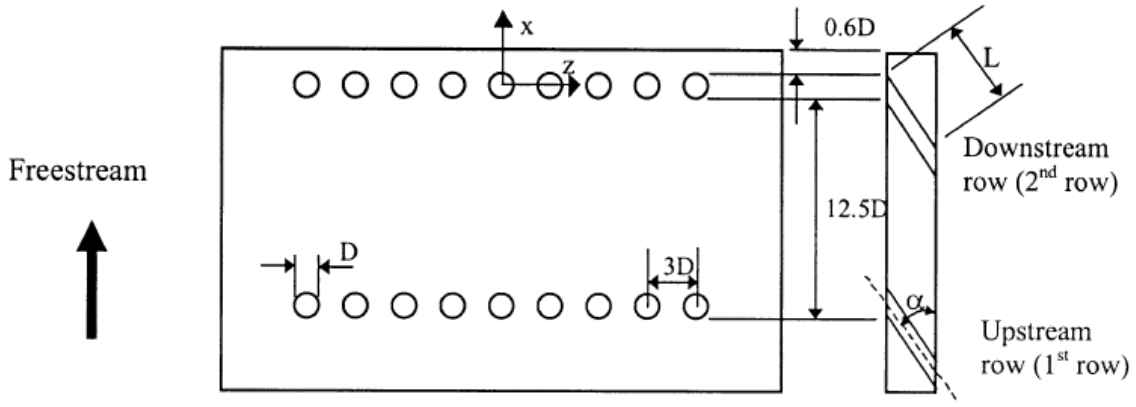

Fig. 1 Flat plate configuration

Table 1 Run cases data

Injection angle	Configurations	P/D	s/D	Blowing ratio
30 , 60, and 90°	One hole		12.5	0.33, 0.5,1.67
	Two inline rows	3	12.5	
	Two staggered rows	3	12.5	

The following assumptions are made:

- Both the hot mainstream gas and the cooling fluid are approximated as air.
- The flow field is symmetrical about the vertical plane passing through the stream wise centerline of a cooling hole (hole-center plane).
- The flow field is symmetrical about the vertical plane passing in the mid-distance between cooling holes (mid-pitch plane).

Mesh Generation

The mesh is generated using GAMBIT®2.3.16. It is crucial that the grid size be as small as possible at boundaries (near flat plate and cooling hole internal walls). It is also important that the grid volumes be as large as possible to reduce the computational time and allocated memory. The grid was non-orthogonal in the tube and near the injection hole. Conservation was maintained by employing control volume concepts similar those employed with unstructured meshes. Figure 2 shows the mesh in more detail.

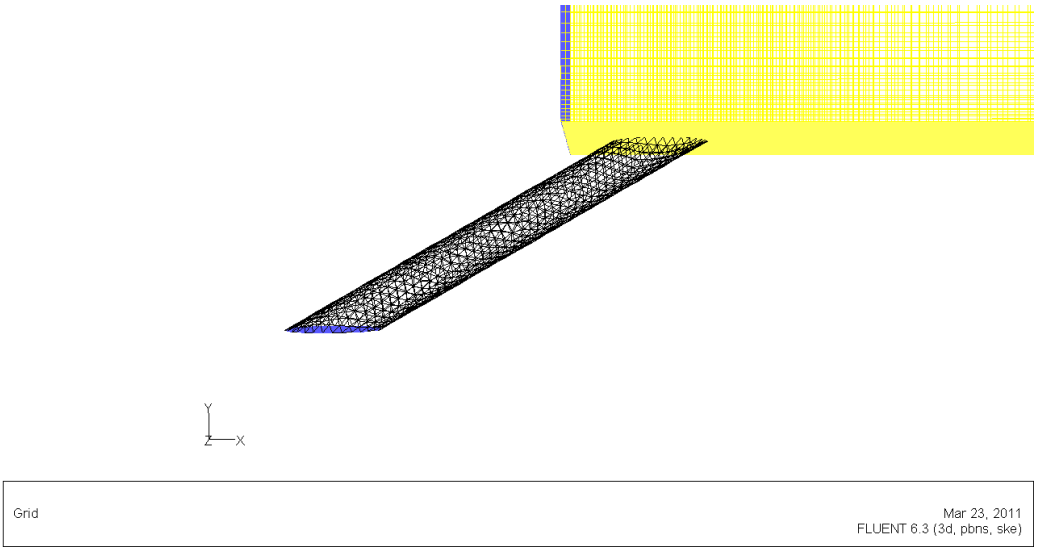

Fig. 2 Mesh generation

Boundary Conditions

The flow field and temperatures in numerical models studied are solved using FLUENT, for the following boundary conditions:

1- Hot main stream inlet

The mainstream gases are approximated as air, with a temperature 333 K. The inlet mainstream flow is considered to have a uniform velocity of 10 m/s. As measured by [14], the turbulence level is 11% and turbulent length scale of 5 mm.

2- Coolant inlet

The coolant inlet is taken to be air, with a temperature 293 K. The inlet coolant flow is considered to have a uniform velocity. Due to the temperature ratio of 333/293, density ratio is maintained at 1.14. According to blowing ratio, cooling velocity inlet can be calculated, as in Table 2.

Table 2 Coolant velocity according to blowing ratio

Blowing Ratio (M)	Coolant velocity (v_c), [m/s]
0.33	**4.29**
0.5	**6.5**
1.67	**21.7**

3- Flat plate

The flat plate surfaces upstream and downstream of the hole injection are considered adiabatic (zero heat flux).

4- Coolant pipe walls

The internal walls of the coolant pipe are considered adiabatic.

5- Periodic boundary conditions

Symmetry boundary condition is applied to the upper boundary of the control volume.

Convergence Criterion

Continuity equation, linear momentum equations and turbulence model (k-ε) equations are solved for the mesh volumes to a residual of 10^{-5}, while the energy equation is solved to a residual of 10^{-6}. The different equations are solved implicitly, for seven configurations applied, for steady state solution using FLUENT6.3.

Verification of Numerical Model

A similar control volume of the same previously- mentioned grid size and type was developed, for verifying numerical model with reference [14]. Comparing the results of the numerical model to the experimental measurements, the results show good agreement of the span wise averaged effectiveness values with corresponding values in the experimental study.

Grid Sensitivity Study

Three models are built, for cooling holes (30, 60, and 90 degree) with the same dimensions illustrated in [14], with three different mesh resolutions. These three models contain different numbers of mesh elements, namely 217998, 598830 and 1253317 elements. Studying the effect on centerline effectiveness of film cooling, the model sensitivity to resolution begins to vanish at the third resolution (1253517 cells) with a maximum error of 5%. To minimize the processing time and allocated memory, this resolution is taken in all configurations of the present studies.

Results

The computational methodology implemented in the present research was developed and validated for studying jet– cross flow interactions as described by C.H.N. Yuen, and R.F. Martinez-Botas, (2005). CFD analysis was performed using Fluent solver and turbulence closure was attained using standard k–ε turbulence model in conjunction with the standard wall functions. The results are classified into the following:

1- Effects of Hole Angles

In this section, the effect of hole injection angle was studied for three angles (30^o, 60^o, and 90^o) and blowing ratio of 0.33.

Figure 3, 5, and 7 shows the contours of effectiveness of single hole of 30^{o} holes and a length -to-diameter ratio of 4 with blowing ratio of 0.33. Also the temperature distribution contours is shown in Figure 4, 6, and 8. It should be noted that values on effectiveness contours can be drawn in the reverse manner to those on temperature contours. That is; a temperature of 333 K corresponds to zero effectiveness and a temperature of 293 K corresponds to an effectiveness of 100%. When plotting contours of temperatures and effectiveness on RGB color scales, a red color on a temperature map will correspond to a blue color on an effectiveness map.

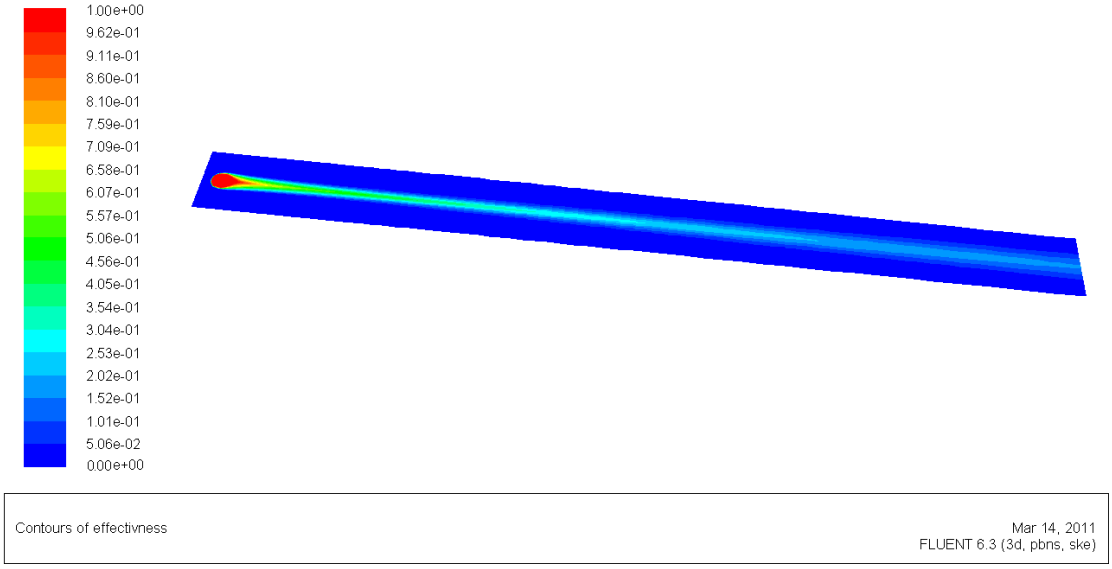

Fig. 3 Contours of effectiveness of single hole of 30°

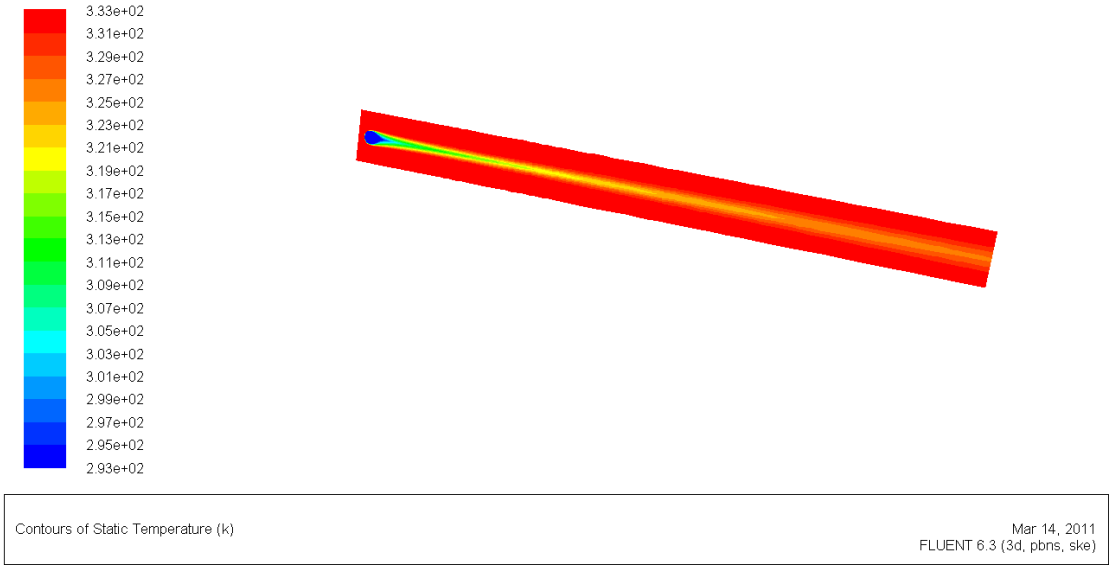

Fig. 4 Contours of temperature with of single hole of 30°

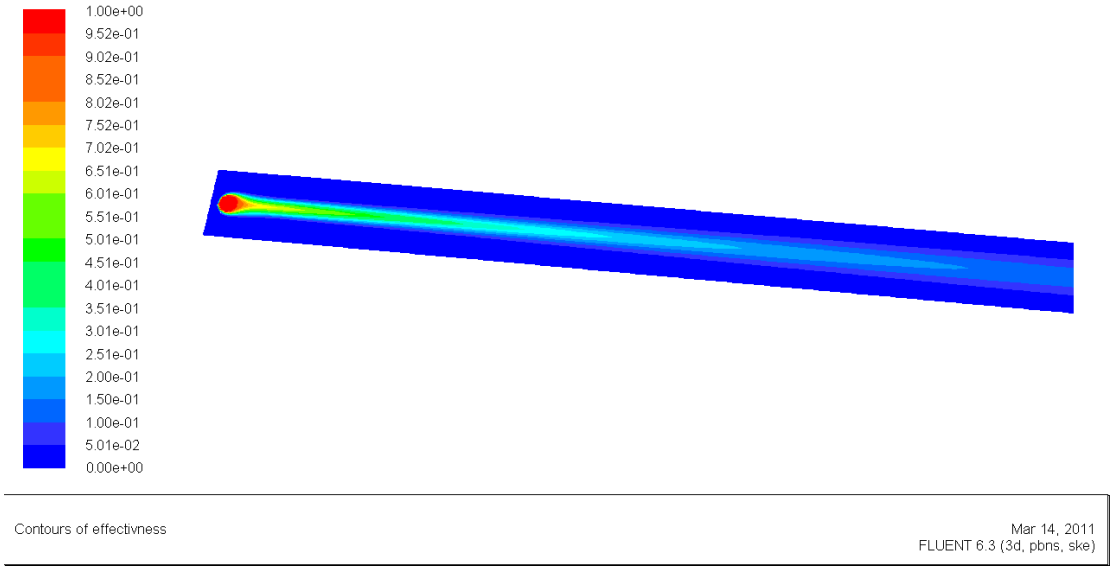

Fig. 5 Contours of effectiveness of single hole of 60°

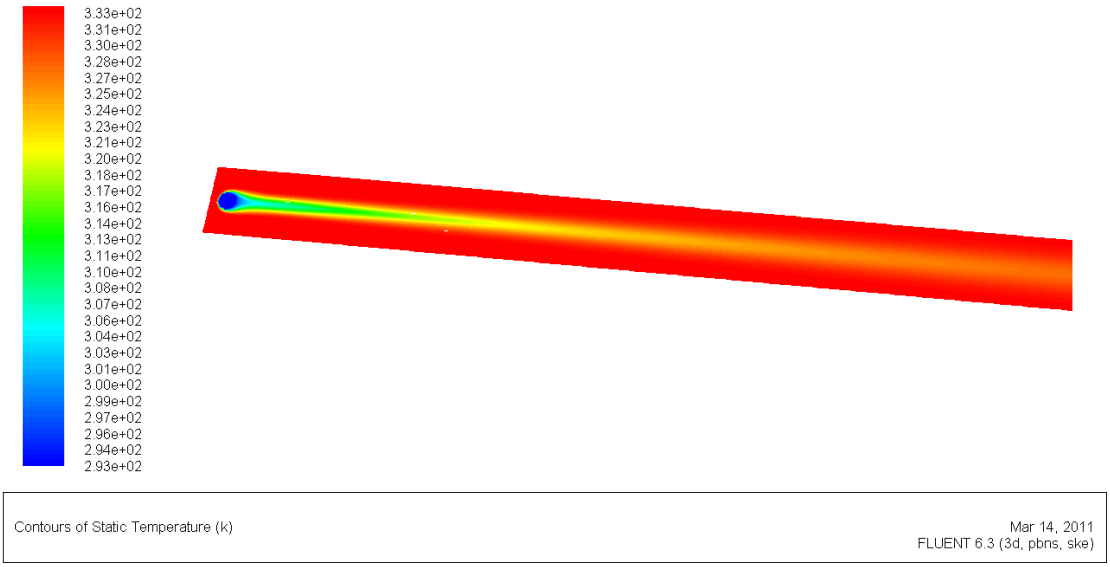

Fig. 6 Contours of temperature of single hole of 60°

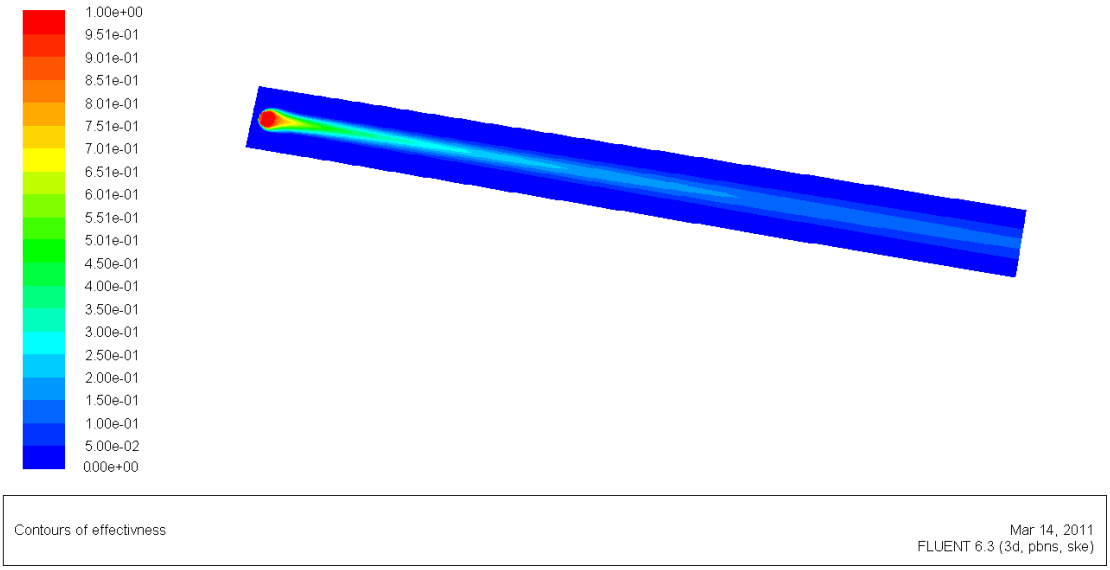

Fig.7 Contours of effectiveness of single hole of 90°

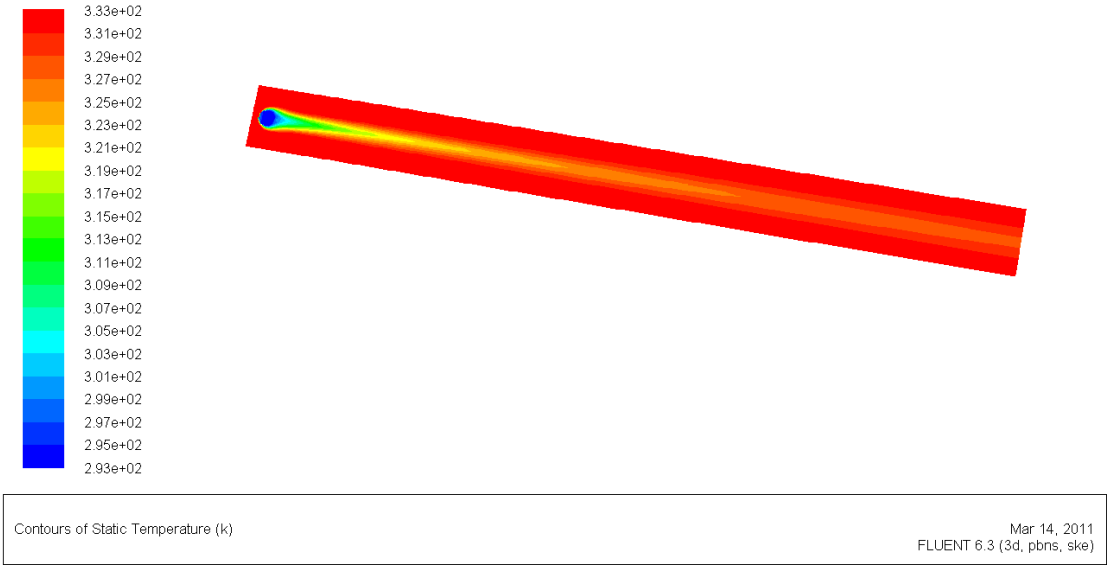

Fig. 8 Contours of temperature of single of 90° hole

The centerline effectiveness distribution is shown in Figures.9,10,and11 the numerical results catch the phenomenon and shows similar trend of experimental results with shifting up due to the bending of the jet by the cross flow which produces large values of the turbulent stresses that lead to significant turbulence production in the near field of the jet. At X/D≥ 30 the simulation and experimental are closely approach, because the wall temperature in this region becomes higher and closer to hot stream temperature.

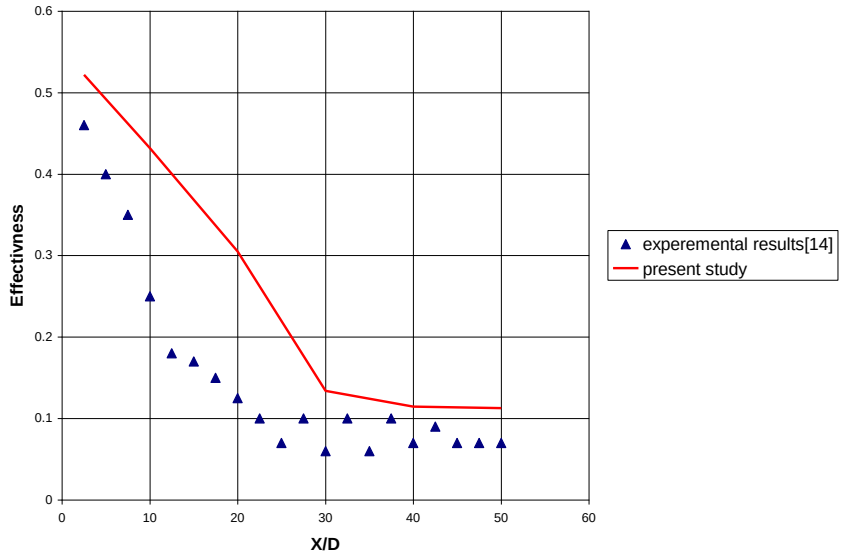

Fig. 9 Centerline film cooling effectiveness of single hole with injection angle30° and blowing ratio: 0.33

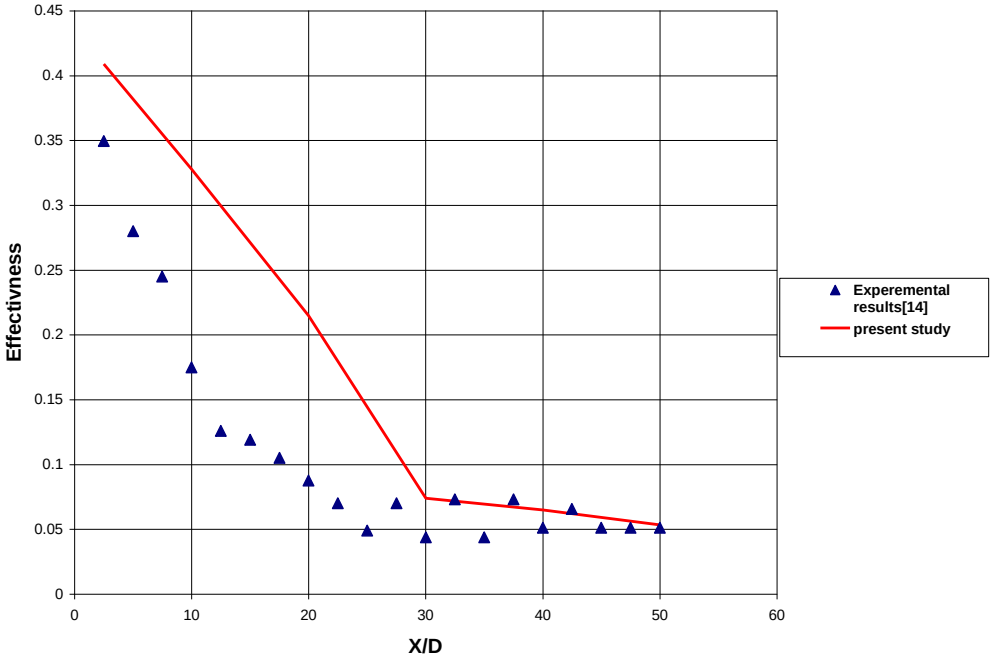

Fig. 10 Centerline film cooling effectiveness of single hole with injection angle 60° and blowing ratio of 0.33

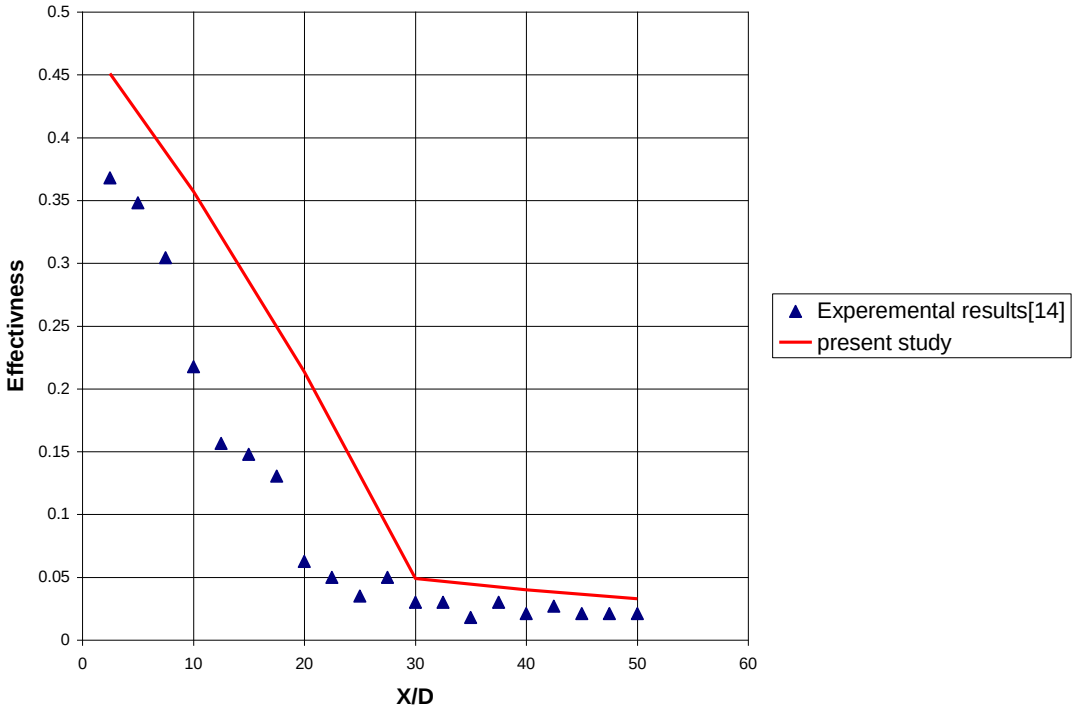

Fig. 11 Centerline film cooling effectiveness of single hole with injection angle 90° and blowing ratio of 0.33

The main observation from this study that the 30^o hole gave larger effectiveness values than 60^o and 90^o at the blowing ratio of 0.33 with the same length-to-diameter ratio. The simulation results have the same trend of experimental results where $\eta_{30^o} \rangle \eta_{60^o} \rangle \eta_{90^0}$.

2- Effect of Cooling Holes Arrangement

In this section the numerical study focused on the holes arrangement by comparing two different arrangements in line and stagger.

Figure 12 shows the contours of effectiveness of inline holes of 30^o injection angle and a pitch-to-diameter ratio of 3 with blowing ratio of 0.33. Also the temperature distribution contours is shown in Figure 13.

The centerline effectiveness distribution of inline row of holes with injection angle of 30^o is shown in Figure 14, the simulation results has the same behavior of experimental results, and at X/D≥ 30 the simulation and experimental are closely approach.

Figure 15 shows the contours of effectiveness of stagger holes of 30^o injection angle and a pitch-to-diameter ratio of 3 with blowing ratio of 0.33. Also the temperature distribution contours is shown in Figure 16.

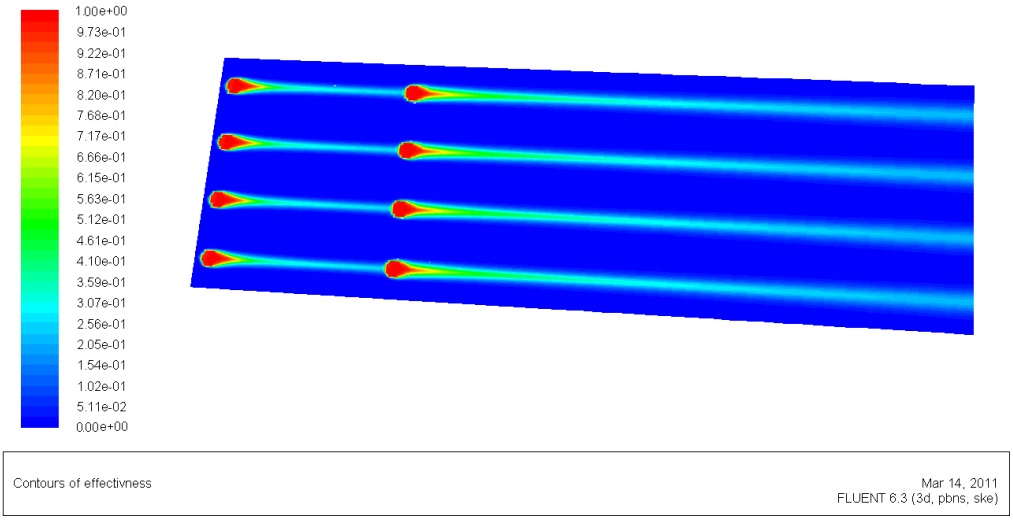

Fig. 12 Contours of effectiveness of inline row of holes with 30° injection angle and 0.33 blowing ratio.

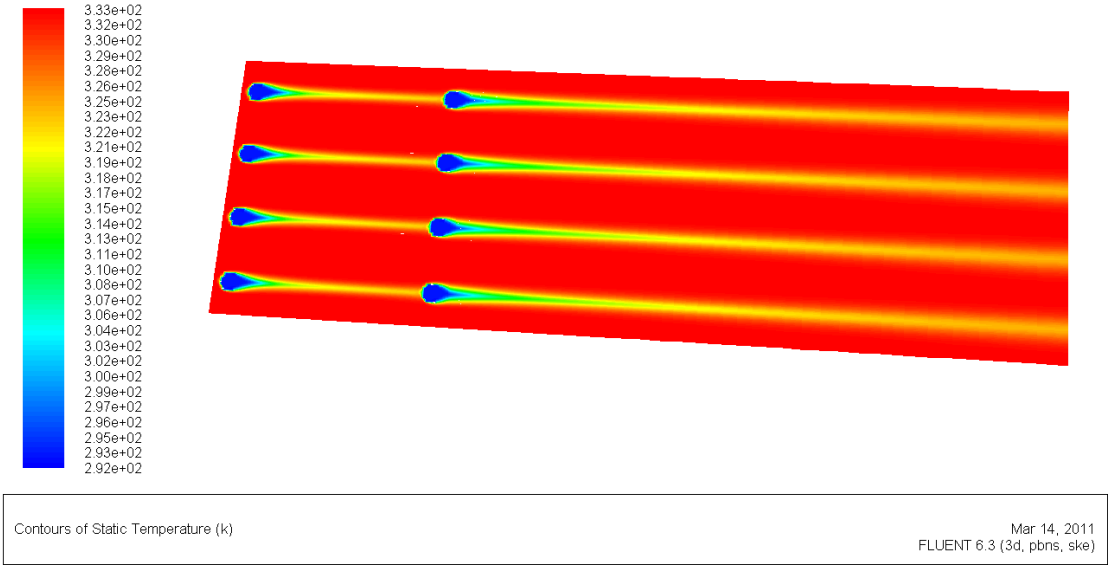

Fig. 13 Contours of temperature distribution of inline row of holes with 30° injection angle and 0.33 blowing ratio.

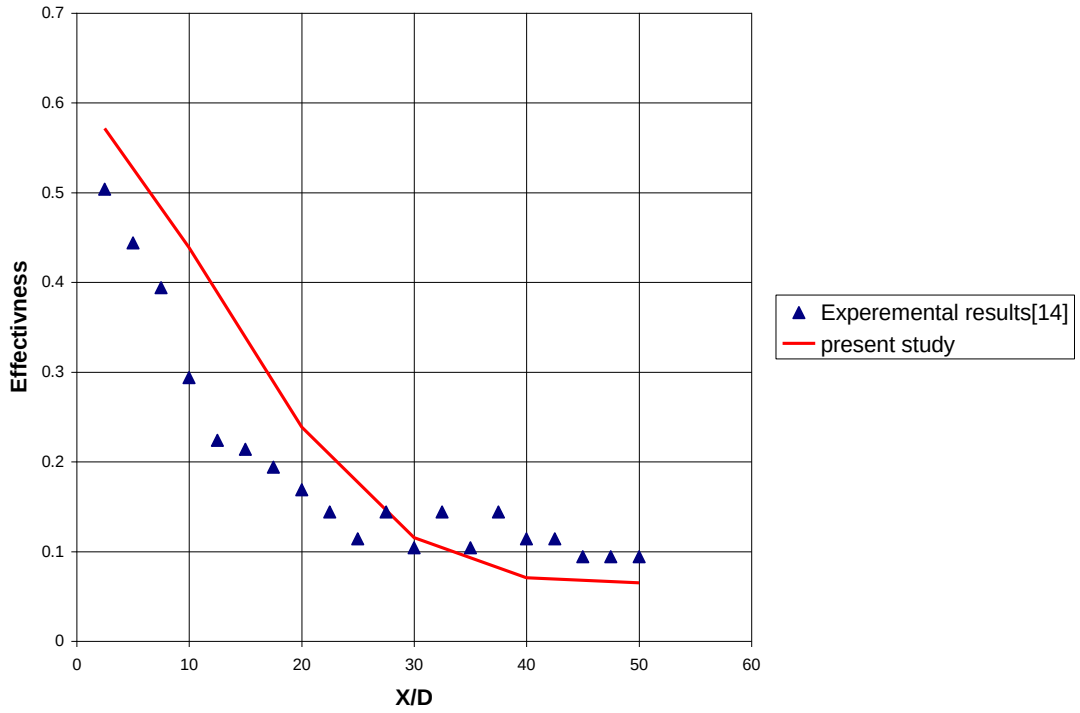

Fig. 14 Centerline film cooling effectiveness of inline holes (p/d=3) with injection angle 30° and blowing ratio of 0.33

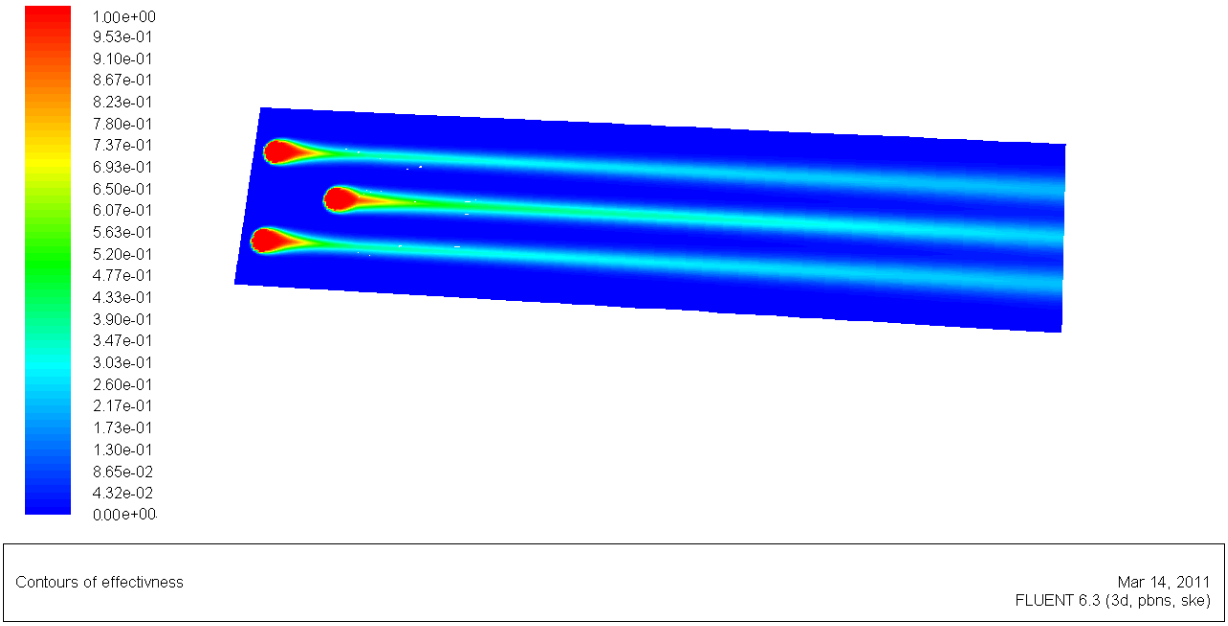

Fig. 15 Contours of effectiveness of stagger holes with 30° injection angle and 0.33 blowing ratio.

The centerline effectiveness distribution of Stagger holes with injection angle of 30^{o} is shown in Figure 17, the simulation results has the same behavior of experimental results with very small shifting up, and at X/D≥ 30 the simulation and experimental are closely approach.

By comparing the previous two results, the effectiveness in staggered holes was similar to those inline rows of the same injection angle, and the effectiveness was decreased.

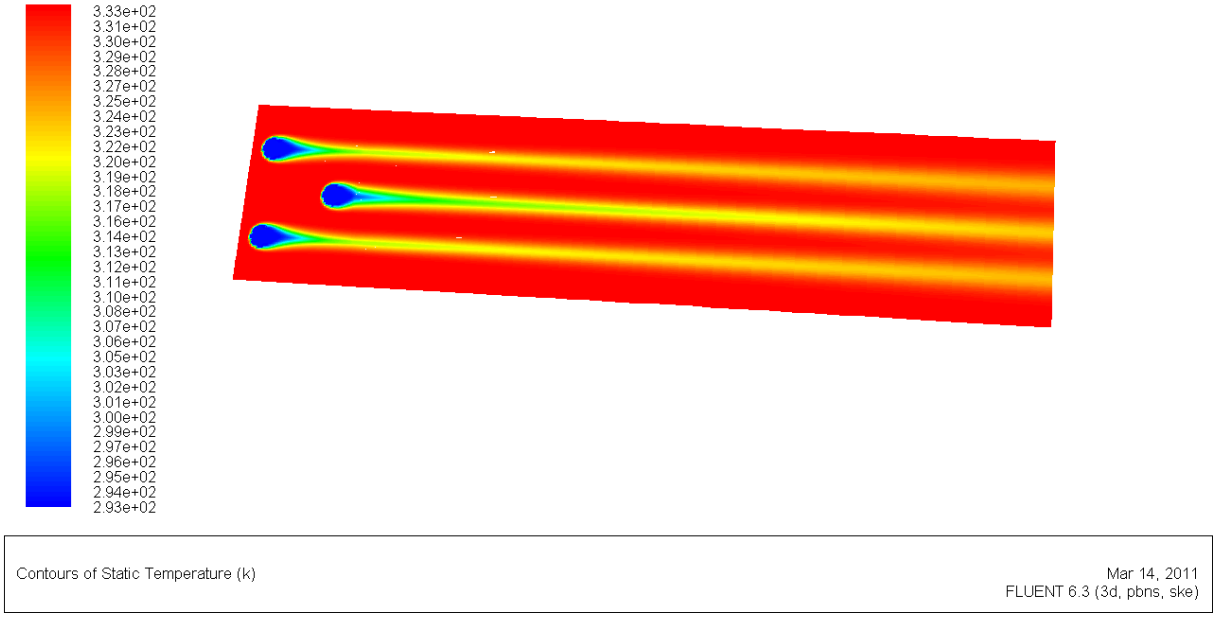

Fig. 16 Contours of temperature distribution of stagger holes with 30° injection angle and 0.33 blowing ratio.

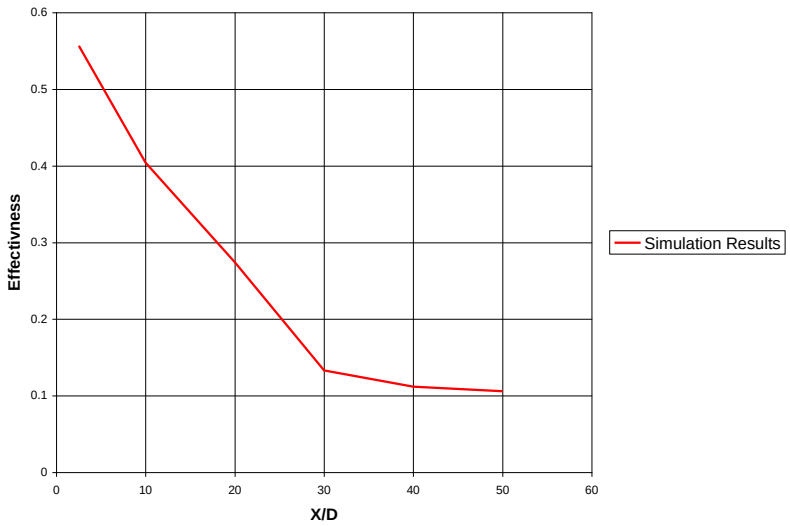

Fig. 17 Centerline film cooling effectiveness of stagger holes (p/d=3) with injection angle 30° and blowing ratio of 0.33.

3- Effect of Blowing Ratio

Effect of blowing ratio on effectiveness is studied, by varying the blowing ratio (0.33, 0.5, and 1.67) in simulation for single hole with injection angle of 30^{o}.The results are shown in figures 18 and 19.

The maximum η was achieved with a blowing ratio of 0.5, and the results shows that the increase of blowing ratio negatively affects film cooling, due to the lift-off effect and the optimum blowing ratio depends on hole injection angle. Figure 20 shows the lift-off phenomenon.

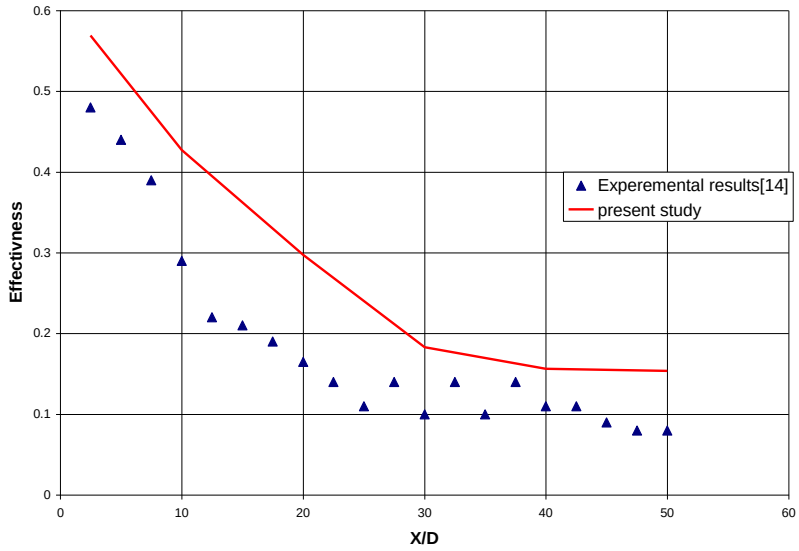

Fig. 18 Centerline film cooling effectiveness of single hole with injection angle30° and blowing ratio of 0.5.

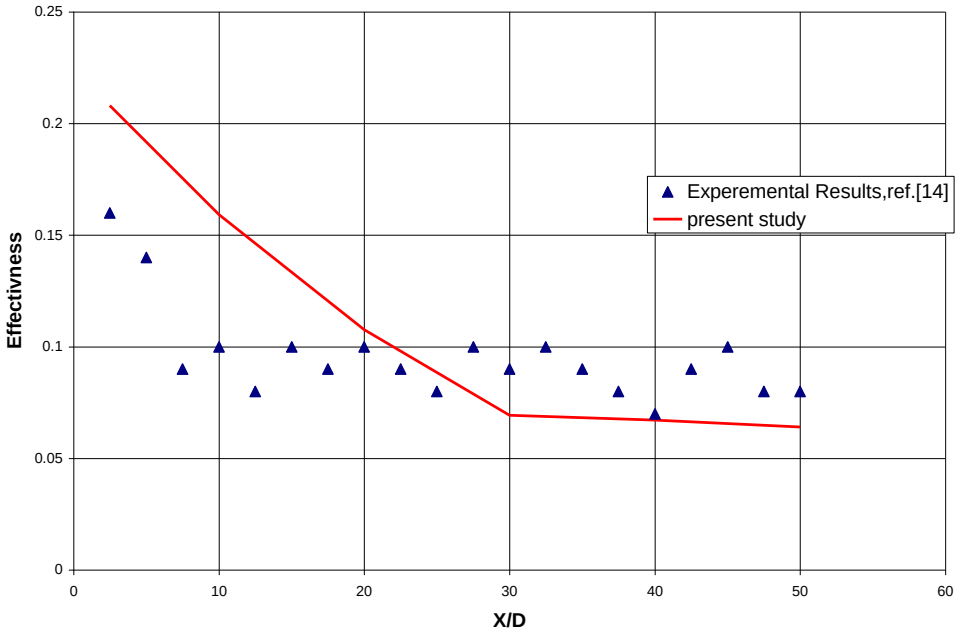

Fig. 19 Centerline film cooling effectiveness for single hole with injection angle30° and blowing ratio of 1.67.

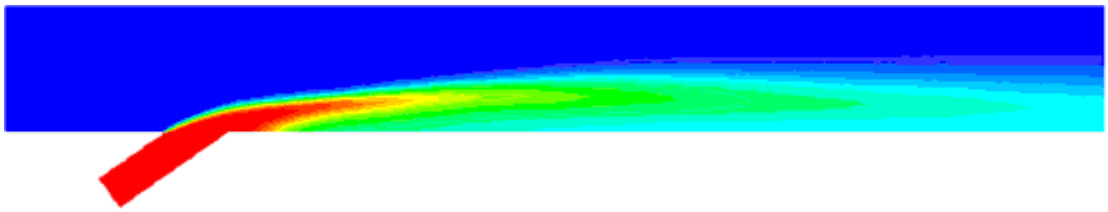

Fig. 20 Lift-off phenomenon.

Conclusion

The computational results were compared with experimental results, and all the results of simulation catches the phenomenon, and indicated good agreement.

- The value of effectiveness and sensitivity is affected by many factors as injection angle, blowing ratio, holes arrangement, etc. that makes film cooling performance study not easy.

- This study indicates that the best hole angle is 30^0 at blowing ratio of **0.33,** where $\eta_{30^o} \rangle \eta_{60^o} \rangle \eta_{90^0}$.

- The optimum blowing ratio for injection angle 30^0 is **0.5.**
- Staggered holes were similar to those inline rows of the same injection angle, and the effectiveness was decreased.

References

1. A.Pashayev, D. Askerov, R. Sadiqov, A. Samedov, and C. Ardil, Modeling and Simulating of Gas Turbine Cooled Blades, World Academy of Science, Engineering and Technology 9, 2005.
2. N.E.Waldren and J.A.Flint, Description of an Experimental High-Temperature Turbine and Associated Test Rig, NACA report 126, 1965.
3. J.F.Barnes, J.E.Northwood, and D.E.Fary, The Behaviour of Extruded Air-Cooled Rotor Blades Subjected to Steady High Temperature and Rotational speed, NACA report 126, 1965.
4. P.Cochran and Robert P. Benglar, Experimental Investigation of Air-cooled Turbine Operating in A Turbojet Engine At Turbine Inlet Temperature up to 2500^o F,NACA Technical Note D-1046, 1961.
5. Jack B. Esgar, Raymond S. Colladay, and Albert Kaufman, An Analysis of The Capabilities And Limitations of Turbine Air Cooling Methods, NACA Technical Note TN D-5992, 1970
6. Peter L. Meitner, Analysis of Metal Temperature and Coolant Flow with a Thermal-Barrier Coating on a Full-Coverage- Film-Cooled Turbine Vane, NACA Technical Paper 1310, pages 78-20, 1978.
7. Wilson B. Schramm, Alfred J. Nachtigall, and Vernon L. Arne, Analytical comparison of turbine blade cooling systems for a turbojet engine, NACA RESEARCH MEMORANDUM, E52J29, 1973.

8. Vernon L. Arne and Alfred J.Nachtigall, Calculated effects of turbine blade cooling on performance of turbojet engine, NACA RESEARCH MEMORANDUM, E51J24, 1972.
9. John M. Farley, Analytical investigation of turbine blade cooling systems for a prototype J47D turbojet engine, NACA RESEARCH MEMORANDUM, E51J113, 1972.
10. Sidney C. Huntley, Effect of compressor air bleed on performance of a centrifugal air flow turbojet engine with a constant-area jet nozzle, NACA Technical Note 2713, 1967.
11. L.R. Woodworth, Significance of major cycle variables on turbojet engine performance at Mach 3.0, NACA RM 1571, 1978.
12. Reece V. Hensley, Frank E. Rom and Stanley L.Koutz, Analytical method of performance evaluation of a turbojet engine with compressor air bleed, NACA Technical Note 2053, 1970.
13, Grzegorz Nowak, Cooling system optimization of turbine guide vane, Applied Thermal Engineering 29, pp.567–572, 2009.
14. C.H.N. Yuen, and R.F. Martinez-Botas, Film cooling characteristics of rows of round holes at various stream wise angles in a cross flow: Part I. Effectiveness, International Journal of Heat and Mass Transfer 48, 4995–5016, 2005.